ChemComm

Pyrolysis-based methods to upcycle plastic wastes to value-added carbons

Journal:	*ChemComm*
Manuscript ID	CC-FEA-05-2025-002765.R2
Article Type:	Feature Article

FEATURE ARTICLE

Pyrolysis-based methods to upcycle plastic wastes to value-added carbons

Received 00th January 20xx,
Accepted 00th January 20xx

DOI: 10.1039/x0xx00000x

Anthony Griffin[a] and Zhe Qiang[a,*]

The ever-increasing production of plastics reveals the necessity of robust waste recycling technologies, which is critical for environmental sustainabilty and economic prosperity. Not only must these processes be capable of addressing a broad variety of commodity polymers, but they must also produce cost-competitive products to allow for widescale implementation. Conversion of plastic wastes into value-added carbon materials offers a promising upcycling pathway, potentially coupling cost-efficacy with process scalability. This work reviews the current progress in plastics-derived carbons, focusing on common commodity thermoplastics such as polyolefins, polyethylene terephthalate, and polystyrene while also highlighting more complex plastic waste streams, including thermosets, engineering plastics, composites, and mixed wastes. Lastly, a perspective is provided on future research opportunities to further enable the upcycling of plastic wastes to valuable carbonaceous materials.

1. Introduction

The massive global production and utilization of single-use plastics has resulted in a unique predicament where plastic waste continues to both accumulate and persist in the environment, leading to various impacts on human and environmental health.[1–4] With more than 460 million metric tons of plastic generated annually and a projected increase to 1.2-1.6 billion metric tons by 2050,[5,6] many strategic approaches have been implemented toward a sustainable plastics economy, including developing efficient recycling methods,[7–9] reducing single-use plastics,[10,11] and building infrastructure for improved waste management.[12,13] Particularly, an enormous amount of effort has been focused over the past decade on developing scalable methods of converting plastic waste into reprocessed/re-engineered products or valuable raw materials, enabling their extended use and lifetime.[14,15]

Historically, landfilling and incineration have been the most prevalent waste management methods for end-of-life plastics, however, they directly lead to microplastic generation/contamination or toxic gas emissions.[8] Mechanical recycling offers a simple approach to recycling a wide range of commercial thermoplastics, though this practice is limited to single-sourced and high-quality waste feedstocks.[16] If waste feedstocks are not properly separated or compatibilized, phase separation between differing plastics leads to poor interfacial adhesion and reprocessed plastics exhibit significantly reduced mechanical properties.[17] Moreover, mechanical reprocessing can cause polymer chain scission and/or crosslinking, which reduces material properties and processability, restricting this method to only a few life cycles of plastics.[18] Additionally, a consistent limitation with mechanical recycling is its inability to address thermoset polymers, excluding a significant portion of total plastic waste.[19,20] While chemical recycling has been demonstrated as an effective route to convert various commodity polymers to chemical building blocks or fuels, sequential use of new products could often result in additional cost and energy, potentially offsetting environmental benefits.[14,21] Another important consideration is that secondary raw materials may not be cost competitive compared to their inexpensive virgin analogs.[22,23]

Chemical upcycling of complex plastic wastes into value-added materials is a promising route to simultaneously address issues related to both recycling and economic feasibility.[24,25] Pyrolysis, or a thermochemical process involving heating under an inert environment, has been demonstrated to produce various advanced materials and/or chemical building blocks from a wide range of plastic precursors.[24,26,27] While toxic off-gases are produced during pyrolysis, these byproducts can be sequestered as well as repurposed as energy sources.[28–30] We note that the processing parameters in pyrolysis can be tuned to modulate the formation of upcycled products; in some literature precedents, slow heating rates can result in increased amounts of char while fast heating rates can favor gaseous or wax-based molecules.[31,32] Recently, several industrial-scale pyrolysis plants have been developed for plastic waste recycling aimed at producing pyrolysis oil, or mixtures of small molecules, which could be used feedstocks for ethylene cracking.[33,34]

Alternatively, conversion of plastic waste into carbon materials can be carried out through pyrolysis.[25,35] We note that advanced carbon materials, ranging from carbon fiber, carbon nanotube, graphene, to porous carbon, could provide enhanced value due to their combination of physical properties that confer excellent performance in various applications.[36–39] For instance, porous carbons, due to their chemical stability, high

[a] *School of Polymer Science and Engineering, The University of Southern Mississippi, Hattiesburg, MS, 39406, USA. E-mail: zhe.qiang@usm.edu*

surface area, and tunable pore texture,[40,41] are a versatile family of materials suitable for various applications, including water remediation,[42–44], biomedicine,[45,46] CO_2 capture sorbents,[40,47,48] catalysts,[49–52] and catalyst supports.[53–55] Moreover, due to their high electrical conductivities and structural stability, carbon materials are heavily used in energy storage, acting as both supercapacitors and electrodes in high-performance devices.[56–58] Owing to their excellent mechanical properties and high strength-to-weight ratio, carbon fibers are often utilized in high-performance composites ranging from aerospace to construction applications.[59] This broad application space is primarily due to the wide range of carbon material properties. For example, carbon-based sorbents exhibit promising performance properties due to tunable pore textures, high surface areas, chemical stability, and their ability to be chemically functionalized such as doping. Electrocatalysts and capacitors can also benefit from high surface areas and tailorable surface chemistries, while leveraging carbon's high electrical conductivity. In comparison, carbon fibers used in structural applications primarily rely on their excellent mechanical properties to maintain structural integrity, and therefore, the presence of pores can result in defective sits which may reduce material strength. The extensive application space for carbon materials and their wide range of critical material properties demonstrates the importance of understanding how carbon synthetic processes and different feedstocks impact final carbon structure and performance. One route of upcycling waste to carbon materials involves mixing plastics with catalyst species followed by catalytic decomposition into gas- or liquid-phase sources, which then interact with catalysts to produce carbon nanomaterials.[60] This concurrent waste degradation and carbon formation pathway has been utilized for preparing carbon nanotubes, graphene, and carbon nanofibers from polyolefins (POs).[35] Specifically, linear low-density polyethylene (LLDPE) can be converted to carbon nanotubes, carbon nanofibers, and amorphous carbon through catalytic carbonization with a nickel (III) oxide catalyst and polyvinyl chloride (PVC) resin, which acts as a source of chlorine radicals to promote LLDPE dehydrogenation and aromatization.[61] In an example of using a sequential approach, plastic waste is first stabilized through a crosslinking reaction to form an efficient carbon precursor. Once plastic waste is thermally stabilized, carbon products are then formed through pyrolysis under an inert environment. Crosslinking of plastic waste can be achieved through thermal treatment under air or through the use of chemical agents to facilitate crosslinking.[25] For instance, Lee et al. utilized thermal oxidation to crosslink LLDPE, allowing its subsequent conversion to graphitic carbon with up to 50 wt% carbon yield.[62] Following thermal oxidation at 330 °C and pyrolysis up to 1200 °C, wastes derived from commercial LLDPE products achieved comparable carbon yields to virgin materials. While several studies have demonstrated heat treatment is capable of stabilizing plastic waste,[63–66] most commercial polymers do not have optimal molecular structures to undergo thermal oxidation-induced crosslinking.[25] To overcome this, chemical agents have been used to promote crosslinking of various commodity plastics.[67] For instance, exposing polyolefin waste to concentrated sulfuric acid at elevated temperatures allows for high degrees of crosslinking and conversion of polymers into efficient carbon precursors.[68,69] Briefly, polymer backbone is functionalized with sulfonic acid groups which then dissociate forming double bonds, followed by a series of additions and rearrangements resulting in intermolecular crosslinking. Thermal stabilization of polystyrene (PS) has also been achieved using carbon tetrachloride (CCl_4) acting as a crosslinker, resulting in hierarchically porous carbons with relatively high surface areas (~679 m^2/g) after pyrolysis.[70] Often, carbonized materials from plastic wastes can be post-functionalized through steps such as surface modification or activation to further improve their performance and functionality for target applications.[71,72] Surface modification involves introducing various species, ranging from metals, small molecules, or polymers, onto the carbon surface to impart varied functionality, while activation uses reactive agents to encourage the formation of micropores within the carbon matrix, and thus increasing surface areas.[73]

While several reviews delve into converting plastic waste into specific carbon nanomaterials for target applications,[32,35,67,73] the intent of this review is to discuss the core aspects of various commodity plastics, and how these distinct polymer structures influence their respective optimal carbonization processes and resulting carbon material properties (Figure 1). Specifically, we will discuss the predominant classes of commercial thermoplastic systems, including from POs, polyethylene terephthalate (PET), and PS, with an emphasis on relations between processing conditions, carbon structure, and performance properties. Following discussion of thermoplastic systems, upcycling of more complex waste feedstocks is covered, including engineering plastics and thermosets. A summary of key upcycling parameters (precursor, carbonization methodology, carbon yield, and target applications) for works discussed is provided in Table 1. Moreover, we provide a brief perspective on the outlook of pyrolysis-based processes for upcycling plastics wastes into carbon materials highlighting future challenges and opportunities.

2. Commodity thermoplastic waste

2.1 Polyolefins

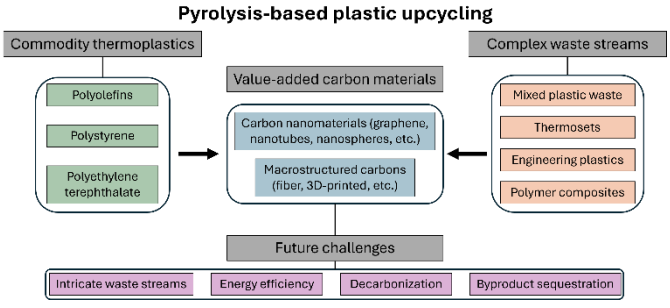

Figure 1. Overview of pyrolysis-based upcycling of commodity thermoplastics and complex waste streams to value-added carbon materials as well as future challenges that must be addressed.

Constituting more than half of global plastic production, polyolefins (POs), including high-density polyethylene (HDPE), low-density PE (LDPE), and isotactic polypropylene (*i*PP), can exhibit tailorable mechanical properties due to decades of advances in synthetic and processing mthods, allowing for precise control of molecular structure and polymer crystallinity.[21,74,75] Briefly, HDPE is linear polymer capable of efficiently packing into zigzag-like orthorhombic crystals granting high degrees of crystallinity, hardness, and tensile strength, whereas LDPE is a type of branched polymer, with lower crystallinity, higher optical transparency, and increased mechanical flexibility. These materials possess significant longevity in the environment after service life that can last at least decades. Currently, only a small amount of PO waste is recycled, with the vast majority still being incinerated or landfilled.[17] Current industrial recycling processes of POs largely rely on mechanical recycling, while a substantial amount of effort is focused on developing scalable chemical recycling routes.[76]

Conversion of POs to carbon structures has been studied for decades, which in general requires an intermediate step of chemical crosslinking. For example, Pennings et al. reacted linear low-density PE (LLDPE) with chlorosulphonic acid at room temperature to achieve high degrees of crosslinking.[68] Upon pyrolysis under tension between 600-1100 °C in an inert atmosphere, carbon fibers with a Young's modulus of 60 GPa and a tensile strength of 1.15 GPa were obtained. Expanding on this approach, Naskar et al. formed hollow carbon fibers by fabricating a bicomponent fiber containing PE and polylactic acid (PLA), which led to patterned structures following PLA removal.[77] To upcycle PO waste streams to carbon materials, Qiang et al. used the sulfonation-based crosslinking method to convert PP-based disposable masks to multifunctional carbon fibers.[78] Specifically, PP fibers were exposed to sulfuric acid at 155 °C for 4 h and then carbonized at 800 °C, resulting in sulfur-doped carbon fibers which exhibited excellent sorbent capabilities for both adsorption of oil and organic dye (basic blue 17). In a follow-up study,[48] PP-derived carbon fibers were utilized for the capture of CO_2 molecules, reaching high adsorption capacities (3.11 mmol/g) and CO_2/N_2 selectivity (>45) primarily due to high affinity of CO_2 molecules to the sulfur heteroatom within the carbon matrix. Furthermore, the conversion of macrostructured POs into carbon materials was investigated using PP-based textile wastes as illustrated in Figure 2a.[79] Through sulfonation-induced crosslinking at 150 °C, fabric wastes with fiber diameters of ~50 µm were able to reach a carbon yield of 59 wt% once carbonized at 800 °C (Figure 2b). Figure 2c shows the intricate woven architectures of the initial fabrics were retained following upcycling to woven carbon fiber mats, with a dimensional shrinkage of ~30%, and the retention of complex microstructure was further confirmed through scanning electron microscopy (SEM) in Figure 2d. These PP-derived carbon mat exhibited excellent Joule heating performance as seen in Figure 2e and 2f. Moreover, Joule heating performance was enhanced, and surface functionality was tuned, by introducing a simple copper electroplating step. Through a similar process, three-dimensional carbon structures

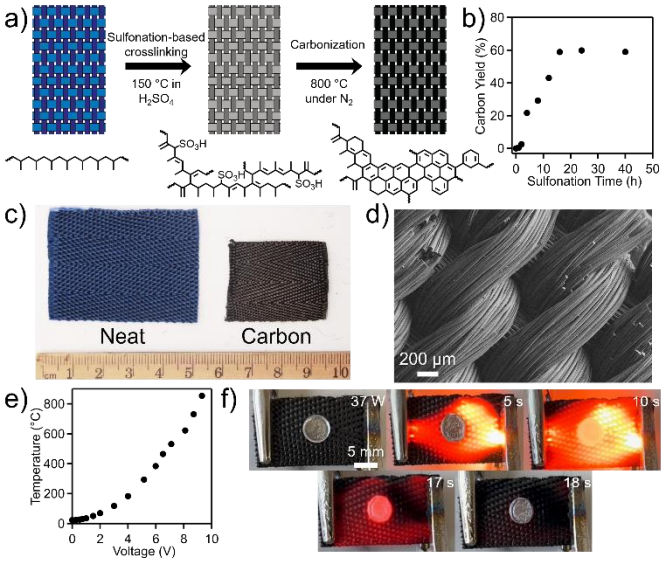

Figure 2. a) Schematic illustration and reaction mechanism for upcycling PP-based textile waste to woven carbon fiber mats through sulfonation-based crosslinking and pyrolysis. b) Carbon yield as a function of crosslinking reaction time. c) Image of textile waste before and after upcycling to carbon. d) SEM micrograph of waste-derived carbon. Joule heating performance of waste-derived electric heating elements: e) Temperature as a function of voltage and f) demonstration of an aluminum pan melting following 10 s at 37 W. Reproduced with permission from ref [79]. Copyright 2023 John Wiley and Sons.

have been achieved by fused filament fabrication (FFF) 3D-printing of PP,[80] PE,[81] and their mixture prior to thermal stabilization and pyrolysis.[53]

Additionally, LDPE-based plastic bags can be upcycled to porous sulfur-doped carbon for lithium-sulfur batteries through microwave-assisted sulfonation,[82] where it was found that the microwave process promotes the sulfonation reaction while also inducing a large number of micropores. Another PE upcycling strategy involved grinding PE plastic bags with basic magnesium carbonate pentahydrate,[83] a flame-retardant agent which acts as a template and also increases PE thermal stability. Following carbonization to 900 °C under a nitrogen environment, hierarchically porous carbons (HPCs) can be obtained after a sequential step of ammonia treatment for simultaneous activation and nitrogen doping. The resulting carbon can serve as electrodes for symmetric supercapacitors, displaying high energy densities (43 Wh/kg) and cycle stability (97.1%) at 2 A/g after 10,000 cycles. The fabrication of straight and helical carbon nanotubes has also been demonstrated through catalytic pyrolysis of PE with maleated PP and ferrocene at 700 °C with a 12 h hold.[84] In this study, PE-derived carbon nanotubes exhibited a total yield of 80 wt%, specifically containing 5 wt% for helical nanotubes, with diameters ranging from 20-60 nm.

2.2 Polystyrene

Polystyrene (PS) is primarily utilized in single-use applications such as food packaging, construction, and insulation materials.[85] Specifically, general purpose PS is a glassy, transparent material largely used in products prepared through extrusion or injection molding processes. In contrast to

the rigid PS, expanded or foamed PS is produced by incorporating blowing agents to expand PS materials to form a closed cell structure consisting predominantly of air (~95%). Through this process, expanded PS becomes highly insulative and lightweight. Moreover, high impact PS (HIPS) with superior toughness can be manufactured by introducing a small amount of polybutadiene (5-10 wt%) rubber that grants higher impact resistance. Despiste some recent work demonstrating the upcycling of PS into high-value small molecules through thermochemical degradation,[86,87] recycling of PS is generally challenging due to high recycling costs as well as low density of expanded PS (which can lead to high transportation cost due to increased volume).[85,88] However, the upcycling of PS waste through pyrolysis can create carbon materials with diverse nanostructures, which might be economically competitive.

In a study by Fu et al.,[70] HPCs were fabricated from PS through a stabilization reaction followed by pyrolysis. By introducing CCl_4, which acted as both a solvent and crosslinker, to PS in the presence of an aluminum chloride ($AlCl_3$) Friedel-Crafts catalyst, a high degree of crosslink density was achieved via carbonyl crosslinking bridges. Upon carbonization, carbon samples with macropores (up to 400 nm), mesopores, and micropores were obtained with a pore volume of 0.66 cm^3/g and a surface area of 679 m^2/g. They found that the PS nanoparticles formed interconnected three-dimensional networks after crosslinking, with this loose aggregation forming macro- and mesopores, and this morphology was retained when converted to carbon. A similar approach using $CCl_4/AlCl_3$ was employed to prepare PS-derived HPCs as anode materials for high-rate lithium-ion batteries,[89] exhibiting stable capacity of 410 mAh/g over 100 cycles. In comparison to amorphous, non-porous carbons, the improved performance from PS-derived HPCs was directly attributed to the hierarchical porosity derived from the crosslinked PS precursor. In another work, Tang et al. investigated the upcycling of PS waste into 3D-HPCs, as shown in Figure 3a.[90] PS waste was first blended with iron(III) oxide (Fe_2O_3), which acts as both a template and catalyst, carbonized at 700 °C for 1 h, and activated with KOH at 800 °C for 1 h, resulting in HPC with a surface area of 2100 m^2/g and pore volume of 3.03 cm^3/g; their microstructure was further investigated through SEM and transmission electron microscopy (TEM) imaging (Figure 3b and 3c). Additionally, PS foam has been demonstrated to form activated carbon through pyrolysis and chemical activation with the absence of intermediate stage of stabilization treatment.[91] Specifically, by dissolving waste PS foam in acetone, drying, and heating to 530 °C with a 10 °C/min heating rate, a carbon char can be formed. Activated carbons with surface area up to 2,712 m^2/g and a pore volume of 1.2 cm^3/g were prepared by activation with KOH, leading to sorbents capable of uptaking methylene blue with a capacity greater than 1 g/g. Another strategy involved using PS microplastics as the starting materials was through stabilization via nitrification and then pyrolyzed with iron (Fe) and molybdenum (Mo) precursors to form bimetallic Fe/Mo-doped sponge carbon for Fenton reaction catalysts with enhanced electron transfer.[92]

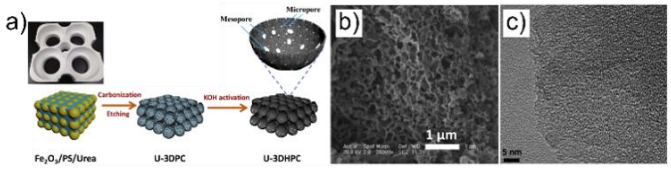

Figure 3. a) Scheme demonstrating PS waste upcycling to 3D-hierarchically porous carbon through carbonization, etching, and activation. b) SEM and c) TEM image of waste-derived carbons. Reproduced with permission from ref [90]. Copyright 2020 Elsevier.

The synthesis of advanced carbon nanomaterials, including carbon nanotubes,[93] carbon dots,[94] carbon microspheres, and graphene, from PS waste have also been demonstrated. For instance, Jou et al. prepared carbon nanotubes from the catalytic pyrolysis of polystyrene at 700 °C in the presence of iron nanoparticles,[93] where it was found that nanotubes with outer diameters from 7.5 to 25 nm can be attained. Specifically for the 25 nm nanotube, an inner diameter of 3 nm was observed indicating a much higher wall thickness than nanotubes prepared through an identical procedure from PP (outer diameters of 16.5-40 nm with wall thicknesses ranging from 3.8-14 nm). The thicker nanotube walls were attributed to the generation of aromatic hydrocarbons during polymer decomposition, in contrast to the aliphatic hydrocarbons from polyolefins, yielding secondary deposition on nanotube surfaces. It is important to note that carbon dots can also be synthesized with high yields (60-85 wt%) from waste PS foams by a solvothermal method in dichloromethane (DCM) and nitric acid at 200 °C for 5 h.[94] Waste-derived carbon dots displayed tunable photoluminescence ranging from white to orange and yellow, allowing for their use as multi-color light-emitting diodes. Furthermore, waste PS cups and commercial PS were converted to solid carbon microspheres (diameters between 4-10 μm) through thermal dissociation at 700 °C under autogenic pressure (~1000 psi),[95] where both feedstocks produced carbon microspheres; however, the waste PS foam cups required a slightly lower time hold (1 h) compared to commercial PS (2 h).

2.3 Polyethylene terephthalate

PET, the most abundant polyester consisting of ethylene glycol and terephthalic acid units, has been extensively utilized for various applications, primarily for single-use packaging and synthetic fibers.[96] Though PET waste has been mechanically recycled for decades, the U.S. recycling rate for PET bottles continues to remain relatively low.[97] In addition, less than 10% of recycled PET is considered commercial-grade usable material due to significant chain scission that occurs during reprocessing.[98] While several examples of chemical recycling of PET down to monomeric species have been demonstrated,[99] upcycling them to carbon nanomaterials can present an economically competitive product.

Various PET waste-derived carbon materials have been developed,[25] the most common of which being porous carbons. For example, waste PET bottles were converted to microporous carbon by first dissolving them in a mixture of DCM and trifluoroacetic acid,[100] electrospinning to PET fibers, stabilizing fibers by heating to 220 °C with a heating rate of 5 °C/min and a 2 h hold, and then carbonizing at 750 °C. The final carbon

exhibited a surface area of 457m^2/g . Ok et al. fabricated porous carbon as CO_2 capture sorbents from PET waste, which was collected from several sources, washed and cut into small pieces followed by pyrolyzing to 600 °C with a 1 h hold.[101] To functionalize the PET-derived carbons, activation was carried out, resulting in high CO_2 adsorption capacities up to 3.28 mmol/g. Through life-cycle and techno-economic assessment, it was determined that this scaled upcycling method can display both economic feasibility and environmental benefits, particularly when using CO_2 as the carbon activation agent. Furthermore, porous carbon cuboids (PCCs) were manufactured from waste PET bottles by first preparing a calcium metal organic framework (Ca-MOF) through solvothermal synthesis of PET waste with calcium chloride at 180 °C for 24 h (Figure 4a).[102] The Ca-MOFs were then pyrolyzed up to 700-900 °C to form the final PCCs. Figure 4b shows the nitrogen physisorption isotherms for the PCCs carbonized at 700 °C, 800 °C, and 900 °C, which all exhibit a type IV isotherm. Pore size distributions derived from density functional theory (DFT) are shown in Figure 4c, where carbons pyrolyzed at all temperatures exhibit pore sizes centered at 0.5 nm, 1.3 nm, and ~12-14 nm. The surface areas corresponding to micropores, mesopores, and macropores are summarized in Figure 4d, where the microporous surface area decreases with higher carbonization temperature, potentially due to pore shrinkage. Additionally, Lee et al. demonstrated the synthesis of porous carbon from PET waste through autogenic pressure carbonization at 600 °C and followed by KOH activation at 800 °C.[103] By decomposing PET bottles in a confined reactor, a series of secondary reactions can take place eventually forming pyrolytic carbon. With a high surface area of 1,931 m^2/g, these PET-derived carbons were used as CO_2 capture sorbents, exhibiting an adsorption capacity of 4.44 mol/kg and a CO_2/N_2 selectivity of 7.99.

Carbon nanomaterials have also been developed from PET waste through a molten salt approach,[104] where PET waste was blended with sodium chloride (NaCl) and heated to 1300 °C under air at 10 °C/min. After removal of salt, graphitic nanosheets were observed with a thickness less than 10 nm, a bulk density of 1 g/cm^3, and a high electrical conductivity of 1150 S/m. Hassan et al. studied the synthesis of graphene from PET waste by heating to 800 °C for 2 h under nitrogen with a catalyst prepared from citric acid combustion of anhydrous iron(III) chloride and aluminum nitrate nonahydrate.[105] The nanostructure of derived graphene was probed using TEM, where single, or a few, layers of sheets were all observed. Furthermore, PET waste from used water bottles were exposed to a rotating cathode arc discharge technique to prepare nanosized, ultrafine solid carbon spheres with an average diametes of 221 nm at lower anode temperatures (1700 °C), whereas elevated temperatures (2600 °C) led to carbon tubules and multiwalled carbon nanotubes (MWCNTs) with an averaged diameter of 364 nm and 20 nm, respectively.[106] Additionally, carbon dots can be prepared from PET textile waste by blending PET with ethylene glycol and exposing to microwave irradiation (540 W) for 20 min.[107] Carbon dots were then fabricated through a hydrothermal approach by blending the unpurified mixture with urea and pyromellitic acid in an autoclave at 260 °C for 24 h. PET-derived carbon dots were found to have an average particle size of 2.8 nm with excitation-independent emission ranging from 340-440 nm and a fluorescence quantum yield of 97.3%.

3. Complex waste streams

3.1 Mixed plastics

Compounding the many issues of thermoplastic recycling, mixed plastics, containing contaminated and comingled waste streams represent an even greater challenge, as conventional mechanical recycling can result in substantially downgraded properties due to weak interfaces from phase separation.[108,109] Various compatibilizers have been developed to improve mechanical recycling feasibility,[17,110–112] while several chemical recycling methods are focused on selectively decomposing specific components down to building blocks.[113,14,114] Recent studies indicate the potential of enabling collective upcycling of comingled plastics to carbon materials.[73,115,116] The feasibility of pyrolysis-based recycling of mixed plastics has been investigated, where studies suggest these processes can be cost-competitive while also reducing environmental impacts and energy use when compared to energy recovery recycling methods.[117,118]

In a recent work, Qiang et al. collected single-use polyolefin wastes, prepared mixed polyolefin blends at various PE and PP compositions, and upcycled them to structured carbons (Figure 5a).[53] Three-dimensionally structured materials were first prepared from mixed plastic wastes through fused filament fabrication (FFF) 3D-printing and converted to carbon through sulfonation-induced crosslinking at 150 °C and pyrolysis at 800 °C. Figure 5b displays the complex structures attainable through this mixed waste-derived carbon monolith fabrication method. Mixed polyolefin blends with varied PE/PP compositions (20:80, 40:60, and 80:20 wt% PP:PE) were investigated, with blends requiring reduced crosslinking reaction times compared to homopolymers, while no impact on resulting carbons were

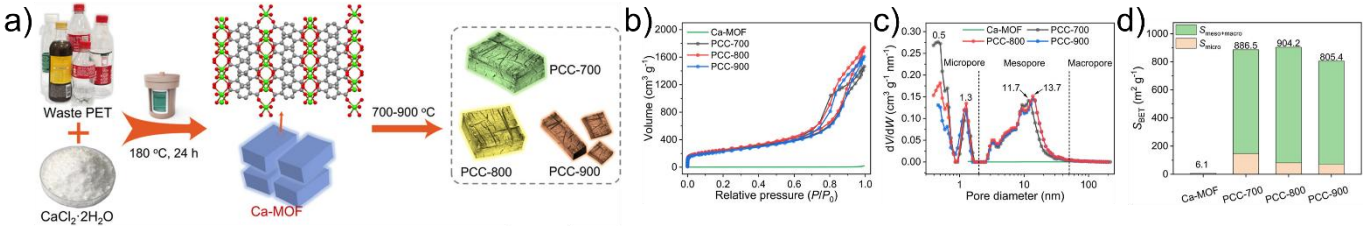

Figure 4. a) Illustration of the conversion of PET waste to porous carbon cuboids through pyrolysis with Ca-MOFs. b) Nitrogen physisorption isotherms, c) pore size distributions, and d) surface areas for PET-derived carbons. Reproduced with permission from ref [102]. Copyright 2022 American Chemical Society.

observed. The accelerated crosslinking kinetics were facilitated by the lower melting temperature of PE (compared to PP) coupled with phase separation between polyolefin components promoting sulfuric acid diffusion. As discussed in previous sections, structured carbons can function as highly efficient Joule heating materials, which can then be implemented as catalyst supports for electrified thermo-chemical synthesis. When utilized for ammonia decomposition for hydrogen production, it was found that conversion increased significantly compared to a conventionally heated (convection heating) system (between 50-250% increase) as shown in Figure 5c. The enhanced catalytic activity was attributed to potential electric field impacts, promoting associative desorption of chemisorption nitrogen atoms as well as localized heating of catalytic nanoparticles. Importantly, life cycle analysis found that global warming impact and life cycle energy consumption associated with Joule-heated hydrogen production powered from renewable energy sources could be decreased to 400% and 200%, respectively, compared to current industrial practices (Figure 5d and 5e). Moreover, Wang et al. compared homopolymer waste with two blends consisting of 0.66:0.21:0.13 PP:LDPE:PS (mass ratio, blend 1) and 0.35:0.4:0.2:0.05 PP:LDPE:PS:PET (mass ratio, blend 2).[119] Following catalytic pyrolysis at 500 °C for 50 min with the presence of bimetallic catalysts (MgO-supported Co-Ni, Fe-Ni, and Co-Fe), mixed plastics exhibited comparable carbon yields (32.6 wt% for blend 1 and 31.2 wt% for blend 2) to bulk PP (30.2 wt%), LDPE (32.0 wt%), and PS (38.3 wt%) while having similar morphologies. Additionally, in-line catalytic decomposition of a mixed plastic waste blend (0.8:0.15:0.04:0.01 PE:PP:PC/PET:metal/wood, mass ratio) was carried out with a nickel-upgraded slug oxide (Ni-UGSO) catalyst at 700 °C with a feed rate of 0.33 g/min with a reaction duration of 2 h.[120] Mixed wastes were found to form carbon nanofilaments, with diameters ranging from 8-90 nm, though the carbon yield decreased by ~10 wt% compared to a bulk HDPE feedstock (56 wt%). Additionally, the carbon nanofilaments were covered by a thin layer of amorphous carbon due to the presence of PET, PS, as well as other organic contaminants.

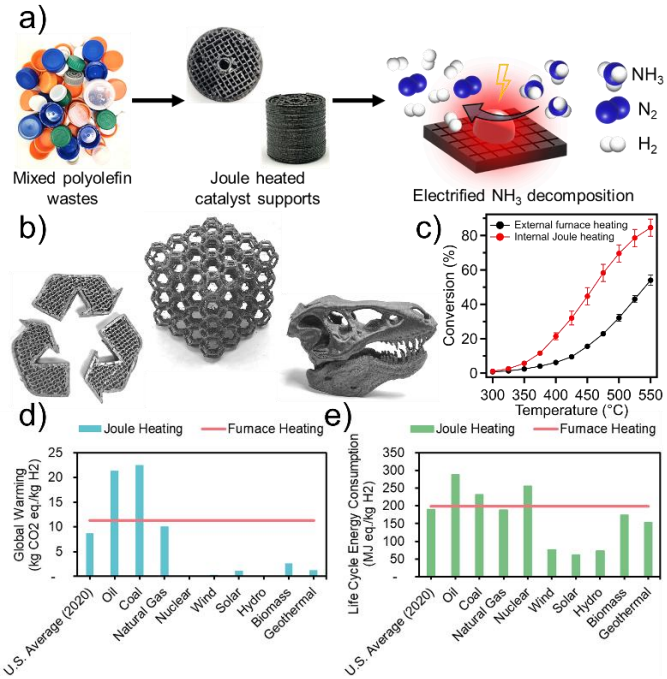

Figure 5. a) Schematic illustration depicting the upcycling of mixed polyolefin wastes to 3D-printed carbon Joule heaters for electrified hydrogen production. b) Images demonstrating the complex carbon macrostructures attainable through FFF-printing. c) NH_3 conversion as a function of temperature for the Joule heated approach compared to a furnace heated analog. d) Global warming impact and e) life cycle energy consumption of Joule-heated hydrogen production. Reproduced with permission from ref [53]. Copyright 2025 The Royal Society of Chemistry.

Fabrication of graphene from mixed plastic wastes has been demonstrated through flash Joule heating (FJH) where mixed waste (0.4:0.2:0.2:0.1:0.08:0.02 HDPE:PP:PET:LDPE:PS:PVC, mass ratio) was ground with 5 wt% carbon black to obtain a conductive material.[121] To provide a brief background, FJH involves passing a direct current between two electrodes across a packed bed of precursor material. The resistance of the material allows the conversion of electrical current directly to heat, capable of achieving very high temperatures (~3,000 °C) within milliseconds. With a carbon content of 81 wt%, the mixed waste blend formed 22 wt% high quality graphene following FJH, only slightly lower than bulk HDPE (27 wt%). Upcycling of mixed plastics (PP:LDPE:HDPE:PS:PET:PVC 0.24:0.3:0.26:0.13:0.04:0.03, mass ratio) to porous carbon sheets has also been demonstrated through pressurized carbonization at 500 °C with magnesium oxide.[122] The majority of carbon growth was attributed to aromatic constituents, with the mixed waste-derived sheets displaying a 33.4 wt% carbon yield, a maximum surface area of 713 m^2/g, and a pore volume of 5.27 cm^3/g. Moreover, porous carbon nanosheets can be produced from mixed plastics through catalytic carbonization on organically-modified montmorillonite (OMMT) followed by KOH activation.[123] Specifically, a blend of 40 wt% PE, 35 wt% PP, 18 wt% PS, 3 wt% PET, and 3 wt% polyvinyl chloride (PVC) containing trace amounts of moisture and ash was blended with OMMT and carbonized to 700 °C for 10 min. The waste-derived carbon nanosheets had high surface areas (up to 2,198 m^2/g) and pore volumes (up to 3.02 cm^3/g) with hierarchical porosity, containing micropores and mesopores (with an average pore size of 3.6 nm). These carbons were then utilized as supercapacitor electrodes, which can show high specific capacitances, such as 207 F/g in aqueous electrolytes and 120 F/g in organic electrolytes at a current density of 0.2 A/g. Furthermore, autogenic pressure pyrolysis of a plastic waste blend, containing 31.6 wt% PP, 31.4 wt% LDPE, 22.1 wt% HDPE, and 11.9 wt% PS, at 700 °C for 30 min with a reactor pressure up to 7 MPa can result in high CH_4 content pyrolysis gas and carbon microspheres (2-8 µm diameters) containing semicrystalline graphitic structures.[124] Noteworthily, this process resulted in negative carbon emissions (-449 kg CO_2-eq per ton of plastic waste), while having 294 kg CO_2-eq in carbon emissions associated with converting wastes into fuels and carbon nanomaterials. Moreover, carbon nanotubes have also been fabricated from mixed plastics (LDPE:PP:PS:PET 0.4:0.4:0.1:0.1, mass ratio) through pyrolysis between 600-800 °C and followed by chemical vapor deposition via the use of nickel-based catalysts.[125] Though carbon nanocages and

MWCNTs could be manufactured, a lower carbon yield was observed at 800 °C for the waste blend (22 wt%) compared to PP (32 wt%) and LDPE (31 wt%) due to PET decreasing hydrocarbon gas reactivity. At lower pyrolysis temperatures (500 °C), carbon yield was much lower for the mixed waste blend (3 wt%) than PP (32 wt%) and LDPE (21 wt%). Altogether, these findings suggest that upcycling mixed wastes to value-added carbons with varied structures and material properties is attainable, while additional fundamental understanding into recycling strategies would be required to address the complexity from blend compositions in real waste systems.

3.2 Thermosets and engineering plastics

Thermoset polymers, with 65 million metric tons generated annually, account for a large fraction of total polymer production (~20%).[126] While permenate crosslinking typically imparts chemical resistance and dimensional stability, its prescence makes thermosets particularly challenging to recycle.[127] With demand anticipated to increase in the coming decades and a broad application space, including aerospace, construction, automotive, and electronics, developing waste management strategies for thermoset materials remains a critical challenge and need.[20] While recycling methods like solvolysis and hydrogenolysis as well as the development of reversible networks have been extensively studied,[19] the vast extent of chemistries, material properties, and compositions within all thermosets and engineering plastics necessitate a robust upcycling approach.[127]

It is worth discussing the role of polymer structure on the resulting carbon material formed. For the majority of thermoplastic waste precursors which exhibit minimal carbon yield without additional intermediate step of chemical treatment, significant variation on final carbon yield and carbon architecture is observed for the same polymer feedstock, indicating these important characteristics are primarily dependent on the chosen crosslinking and carbonization strategy (see Table 1). Though carbonization processes and the feedstock's elemental composition are key aspects to consider when upcycling to carbon materials, it should also be noted that initial macrostructures of plastic product could being retained (such as foamed morphology). When considering engineering plastics or thermosets that can be directly pyrolyzed to carbon materials via a one-step process, the polymeric backbone plays a key role in dictating carbon yield in addition to the carbonization method. For example, carbon yields of common precursors include ~20 wt% for crosslinked PS,[128–130] ~45% for polyfurfuryl alcohol,[131] and 40-65 wt% for polyacrylonitrile.[132] Several model thermosets and engineering plastics, with varied polymer backbones, degrees of crosslinking, and resulting carbon yields are discussed below.

Crosslinked polyurethane (PU) foams, due to their nitrogen content and interconnected porous structure, are a promising waste stream for upcycling to carbon materials with open porosity.[133] Wang et al. demonstrated the upcycling of PU foam waste to nitrogen-doped porous carbons and their implementation as polysulfide reservoirs for lithium-sulfur batteries.[134] Foam fragments, mixed with potassium carbonate (K_2CO_3), were directly carbonized at 800 °C for 1 h to form carbons with an interconnected porous, sheet-like morphology and a high surface area (1,315 m^2/g) and nitrogen content (7.2 at%). When employed as a sulfur host for preparing lithium-sulfur batteries, the device achieved high capacities (766 mAh/g) at 0.1C after 100 cycles and high-rate performance (466 mAh/g) at 5C after 100 cycles. Production of graphitic 1D materials from PU waste has also been reported through a FJH technique.[135] Ferrocene and iron(III) chloride-based catalysts were mixed with polymer feedstocks and underwent FJH (0.05-3s) up to 2726 °C. Compared to HDPE-derived graphitic 1D materials, PU-derived carbons exhibited similar morphologies and properties while also retaining nitrogen heteroatoms in the framework (~1.4 at%). PU foam can also be upcycled to porous carbons through autogenic atmosphere pyrolysis under ambient condition at 700 °C for 30 min with a 5 °C/min heating rate, followed by a step of KOH activation at 700 °C for 1 h.[136] Furthermore, upcycling of crosslinked PE foams into porous carbons for CO_2 sorbents has been achieved by crosslinking with fuming sulfuric acid, reaching high degrees of crosslinking (resulting in ~50 wt% carbon yield) within 30 min.[137]

Phenolic resins, a mature class of thermoset prepared from the condensation of phenol with formaldehyde under basic conditions, have long been used as carbon precursors due to their ability to reach relatively high char yields (30-55 wt%), and processability prior to curing.[138–140] In general, phenolic resin is a recognized class of carbon precursor, with broad uses in electronics, coatings, and composites.[141] Upcycling of phenolic resin waste into activated carbon was demonstrated through a microwave-assisted carbonization method,[142] where raw waste was blended with either KOH or phosphoric acid (H_3PO_4) prior to microwave irradiation (500 W) for 30 min. The KOH activated phenol waste-derived carbon was found to have a surface area of 924 m^2/g and relatively low potassium content (0.21 wt%), whereas the H_3PO_4 activated sample exhibited a lower surface area 272 m^2/g and a high phosphorus content (6.1 wt%). Interestingly, activated carbon prepared through pyrolysis using an electric furnace exhibited much lower phosphorus content (1.2 wt%) while no change was observed in potassium content. This was attributed to the high dielectric constant and dielectric loss of the H_3PO_4 activated sample leading to greater microwave irradiation catalyzed H_3PO_4 interactions, and in turn the more rapid carbonization process can kinetically trap a greater content of heteroatom in the final carbon framework.

Additionally, polybenzoxazines represent another family of advanced thermoset resins, prepared through oxazine ring-opening polymerization, which can have fairly high char yields (35-75 wt%) due to their extensive hydrogen bonding throughout their backbone coupled with high aromatic contents.[140,143,144] Nebhani et al. investigated the fabrication of nitrogen-doped carbons for high-performance supercapacitors directly from biosourced polybenzoxazine thermosets.[145] Samples were first cured under air at 150-200 °C between 4-8 h followed by heating to 600 °C, with 30 min holds for every 100 °C interval. Polybenzoxazine-derived carbon was found to have nitrogen loading ~5 at% and a specific capacitance of 700 F/g at

a current density of 10 A/g. Moreover, poly(ether ether ketones) (PEEKs) are a class of engineering polymers utilized in high performance applications due to their high mechanical strength, chemical resistance, and thermal stability.[146] As these high performance polymers typically require high processing temperatures, conventional recycling methods are often ill-suited to address these engineering plastics. Though the upcycling of PEEK waste has not been directly studied, PEEK has been demonstrated as an efficient carbon precursor. For example, Liu et al. investigated the synthesis of microporous carbons by carbonizing PEEK under argon gas up to 900 °C with a 10 °C/min heating rate followed by changing atmosphere to steam or CO_2 gas for activation,[147] resulting in carbons with high surface areas (~3,000 m^2/g) and pore volumes (1.7 cm^3/g). The PEEK-derived carbons were then used for hydrogen storage devices where they displayed volumetric and gravimetric hydrogen storage capacities of 35 g/L and 5 wt%, respectively at 20 bar and -196 °C. In a similar approach, high performance supercapacitors with a capacitance of 237 F/g and excellent cycling stability after 6000 cycles (~93% retention) were developed from using two-layered films of PEEK-derived microporous carbons and reduced graphene oxide, acting as both a binder and active electrode material.[148] It was found that the layered structure, compared to a blended composite film, improved ion accessibility to the hydrophilic microporous carbons and established conductive paths through the graphene oxide network. Furthermore, carbon fiber-reinforced silicon carbide (C/C-SiC) can be fabricated through a liquid infiltration method with polyetherketoneketone (PEKK),[149] another high-performance thermoplastic,[150] and PEEK powders acting as carbon precursors. Though the carbon yield of PEKK (65 wt%) was found to be slightly higher than PEEK (54 wt%), primarily attributed to PEKK's greater crosslinking potential, both PEKK- and PEEK-derived C/C-SiC displayed comparable Young's modulus (40 GPa), strain to failure (>0.55%), and mean flexural strength (>200 MPa). While the conversion of many more high-performance engineering plastics to functional carbon materials have been reported,[151–154] upcycling their waste streams and the underlying impacts of conversion processes on carbon yield and formation still need to be further investigated.

3.3 Polymer composites

Polymer composites, containing functional or reinforcing agents within the polymer matrix, are an essential material class across various industries, such as electronics, construction, and water remediation.[59,155] Significant efforts have been focused on enhancing performance and properties of various composite systems, often by optimizing filler orientation, distribution, and adhesion to the matrix;[156] although, the presence of multiple components make composite recycling quite challenging.[157,158] With increasing demand for polymer composites, these difficult-to-recycle waste streams possess environmental concern, though they also hold economic potential stemming from their valuable and high-performance filler materials.[59] From carbon fiber-reinforced polymer (CFRP) composites alone, it is expected that waste from end-of-life wind turbine blades and commercial aircraft will reach 483,000 tons and 500,000 tons by 2050, respectively.[159,160] The majority of polymer composite recycling methods primarily focus on extracting fillers (typical high value components) from the lower-value polymer matrices. For example, direct pyrolysis of polymer composites between 300-750 °C has been frequently shown to decompose matrices and allow for recycling of filler materials.[161–163] A drawback of this strategy is not only can the matrix material not be recycled, but recovered fillers often have reduced performance properties, due to carbon residues remaining on filler surfaces which require chemical decomposition or burnout under aerobic conditions. For instance, a carbon fiber-reinforced epoxy-amine network was recycled by exposing the composite to monoethanolamine (MEA) with 10 wt% KOH at 160 °C for 90 min.[164] In a binary alkaline solution, the epoxy-amine networks were degraded up to 98 wt% while the carbon fibers retained 93% of their initial tensile strength and elastic modulus. Additionally, carbon fiber-reinforced polyester composites have been recycled by hydrolysis with 80% hydrazine hydrate with NaOH along with a Fenton reaction at 100 °C, where reclaimed fibers kept the morphology, chemical structure, and tensile strength of their virgin analogs.[165] Recycling of epoxy-based composites have also been investigated through several pathways, including thermal decomposition with molten KOH at ~300 °C for 1 h,[166] phosphoric acid catalytic degradation at 250 °C for 1 h,[167] and treatment with peracetic acid at 65 °C for 4 h.[168] While these strategies result in filler extraction from polymer composites with retention of mechanical properties, the bulk of the composite is still not recycled. Aiming at simultaneously recovering carbon fiber and upcycling bismaleimide (BMI) resin from a composite material, Hou et al. developed a chemical degradation approach with acetic acid/calcium nitrate ($Ca(NO_3)_2$ catalytic system at 240 °C for 10 h.[169] Figure 6a shows images of recycled carbon fiber and nitrogen-doped carbon derived from BMI degradation products. Carbon fiber extracted from BMI composites with $Ca(NO_3)_3$/acetic acid (CF-3) was

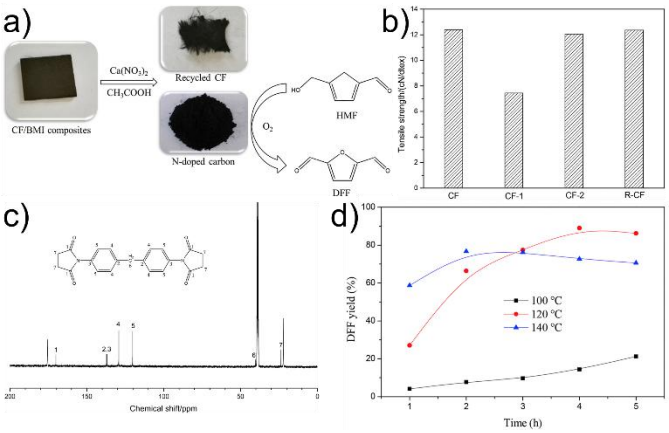

Figure 6. Chemical recycling of BMI-carbon fiber composites. a) Images of recycled products, b) tensile strength of virgin (CF) and recycled carbon fiber (CF-1: Virgin CF treated with $Ca(NO_3)_3$/acetic acid, CF-2: Virgin CF treated with $Al(NO_3)_3$/acetic acid, and CF-3: CF extracted from BMI composites with $Ca(NO_3)_3$/acetic acid), c) ^{13}C NMR of BMI degradation products, and d) DFF yield as a function of reaction time and temperature. Reproduced with permission from ref [169]. Copyright 2020 Elsevier.

found to have comparable tensile strengths to virgin CF prior to treatment (CF) and following treatment with $Ca(NO_3)_3$/acetic acid (CF-1) and $Al(NO_3)_3$/acetic acid (CF-2) (Figure 6b). While the virgin CF's tensile strength declined dramatically following treatment (from 12.42 cN/dtex to 7.42 cN/dtex), the CF extracted from BMI composites had minimal decline (12.32 cN/dtex) due to BMI resin acting as a barrier and reducing CF contact time with the catalytic system. BMI resin degradation products were then separated from carbon fibers and characterized through ^{13}C Nuclear Magnetic Resonance spectroscopy (NMR) as depicted in Figure 6c, where the obtained oligomers' carbon skeletal structure maintained integrity. These results suggested the C-N bonds were cleaved from the catalytic system. Though the reclaimed oligomers lost C=C functionality, they retained nitrogen heteroatoms and could function as nitrogen-doped carbon precursors. BMI resin degradation products were then blended with potassium carbonate, and carbonized to 800 °C for 2 h. Subsequently, BMI-derived porous carbons were used as catalysts for the aerobic oxidation of 5-hydroxymethylfur-fural (HMF) to 2,5 diformylfuran (DFF), which displayed up to an 89 wt% yield at 120 °C following 4 h (Figure 6d). Upcycling of carbon fiber-reinforced epoxy composites has also been demonstrated through plasma treatment,[170] through exposing graphene supported on an alumina fiber porous material to microwave irradiation. It was found that the high temperature generated from plasma converted the polymeric network to combustible gas while also improving the graphitization degree of reclaimed carbon fibers.

4. Outlook and Conclusions

Though the upcycling of plastic waste into carbon materials has been studied for a few decades, its industrial implementation is relatively recent and still an ongoing effort. Looking forward, there remain several challenges that must be addressed to expand the utility of this approach and enable its large-scale application. A critical issue to address is the sequestration of toxic off-gasses during pyrolysis. While these byproducts can be used as energy sources, efficient capture and storage technologies would further enhance the efficacy of this strategy by increasing recycling and decarbonization impacts. Another major challenge is the necessity to enable energy efficiency in pyrolysis process, as high temperature treatment is often involved. Specifically, similar to industrial chemical syntheses of commodity chemicals, including ammonia, hydrogen, and methanol, which require high reaction temperatures, pyrolysis of plastic waste is a highly energy-intensive process that can result in large CO_2 emissions as well as costs associated with process heat.[171] Significant efforts have been focused on developing processes that are economically viable while simultaneously reducing emissions. Several life cycle analyses (LCA) and techno-economic assessments (TEA) have investigated the thermochemical recycling of plastic wastes into small molecules feedstocks and oils, where pyrolysis has been found to potentially be the most profitable strategy compared to gasification, hydrothermal liquefaction, and catalytic processes (hydrocracking and hydrogenolysis).[172] When considering CO_2 emissions, pyrolysis can be more environmentally friendly than a few processes (gasification and hydrothermal liquefaction) though other processes (such as hydrogenolysis and hydrocracking) could have further reduced environmental impacts. Key barriers that hinder pyrolysis upcyling include use of nitrogen gas, energy costs, and inadequate carbon capture technologies. Similar LCA and TEA investigations into the upcycling of PET waste into porous carbon CO_2 sorbents have found that these processes hold potential for financial viability and the possibility of carbon neutrality when scaled up to industrial levels.[101] As mentioned previously, mixed plastics wastes (PP:LDPE:HDPE:PS) were converted to a combination of pyrolysis gas and carbon microspheres through autogenic pressure pyrolysis. It was found that this process exhibited negative carbon emissions (-449 kg CO_2-eq per ton of plastic waste(that outweighted the carbon emissions from the pyrolysis process (294 kg CO_2-eq),[124] the majority of which stemming from energy losses. One strategy that circumvents this issue is through enabling the electrification of heating process, which can be integrated with renewable energy sources to potentially produce a zero-carbon heating solution. As an example, a Joule-heated approach that utilizes a resistive heating element, can allow for the direct conversion of electricity to heat.[173,174] Through this efficient heating method, high reaction temperatures can be reached quickly, resulting in process intensification with smaller required reactor volumes, reduced environmental impacts, and lower process heat inputs. Another advantage of this electrified process is rapid reactor start-up and shutdown speeds, granting adaptability to fluctuating waste feedstock and electricity availability.[175,176] Life cycle analyses of plastic waste upcycling to graphene through FJH have indicated noticeable environmental improvements and reduction in energy usage compared to conventional recycling methods.[177] Microwave-assisted pyrolysis has also been investigated as an alternative for plastic waste upcycling method that can significantly reduce energy consumption and global warming impacts.[178] Furthermore, development of pyrolysis strategies that can readily incorporate a broad range of mixed plastics in addition to engineering high-throughput and continuous material sorting, pretreatment, and feeding pathways will be critical. Upcycling methods for intricate waste streams like copolymers, including both random copolymers, such as acrylonitrile butadiene styrene (ABS), and block copolymers, such as styrenic thermoplastic elastomers, must also be developed due to their high production volumes as well as their valuable morphological features. As demonstrated with several foam waste feedstocks, structured wastes can be valuable as they can be converted to unique carbon materials, if macroscopic geometries can be retained. Additionally, nanostructured feedstocks, such as polystyrene-*block*-poly(ethylene-*ran*-butylene)-*block*-polystyrene (SEBS), presents a distinct precursor that can directly generate carbon materials with mesoporous morphologies.[179,180]

In conclusion, increased generation of plastic waste remains a global issue that threatens both the environment and biological life. To properly confront this grand challenge,

significant technological development is required involving robust recycling strategies that can incorporate complex plastic waste feedstocks at scale. Moreover, to ensure economic viability and scaled implementation, recycled products must match, if not exceed, the market value of virgin materials (i.e. waste precursors). Upcycling of plastic waste into value-added materials has been demonstrated through several approaches, enabling the production of carbon materials with versatile nanostructures, including carbon nanotubes, graphene, and carbon fiber. This review summarizes the conversion of commodity polymers into carbon materials with tailored structures and properties using different processing methods, and offers a brief outlook on future technologies to enable industrial-scale plastic waste upcycling to carbon materials.

Conflicts of interest

There are no conflicts to declare.

Data availability

No primary research results, software or code have been included and no new data were generated or analysed as part of this review.

Acknowledgements

This project was supported by National Science Foundation under grant #CMMI-2239408 and #OIA-2316351.

Notes and references

1 L. Li, J. Zuo, X. Duan, S. Wang, K. Hu and R. Chang, *Environ. Impact Assess. Rev.*, 2021, **90**, 106642.
2 S. Chawla, B. S. Varghese, C. A, C. G. Hussain, R. Keçili and C. M. Hussain, *Chemosphere*, 2022, **308**, 135867.
3 S. S. Shetty, D. D, H. S, S. Sonkusare, P. B. Naik, S. Kumari N and H. Madhyastha, *Heliyon*, 2023, **9**, e19496.
4 R. Kumar, C. Manna, S. Padha, A. Verma, P. Sharma, A. Dhar, A. Ghosh and P. Bhattacharya, *Chemosphere*, 2022, **298**, 134267.
5 OECD, *Global Plastics Outlook: Policy Scenarios to 2060*, Organization for Economic Cooperation and Development, 2022.
6 J. Zheng and S. Suh, *Nat. Clim. Chang.*, 2019, **9**, 374–378.
7 H. Li, H. A. Aguirre-Villegas, R. D. Allen, X. Bai, C. H. Benson, G. T. Beckham, S. L. Bradshaw, J. L. Brown, R. C. Brown, V. S. Cecon, J. B. Curley, G. W. Curtzwiler, S. Dong, S. Gaddameedi, J. E. García, I. Hermans, M. S. Kim, J. Ma, L. O. Mark, M. Mavrikakis, O. O. Olafasakin, T. A. Osswald, K. G. Papanikolaou, H. Radhakrishnan, M. A. Sanchez Castillo, K. L. Sánchez-Rivera, K. N. Tumu, R. C. Van Lehn, K. L. Vorst, M. M. Wright, J. Wu, V. M. Zavala, P. Zhou and G. W. Huber, *Green Chem.*, 2022, **24**, 8899–9002.
8 J. Chen, J. Wu, P. C. Sherrell, J. Chen, H. Wang, W. Zhang and J. Yang, *Adv. Sci.*, 2022, **9**, 2103764.
9 L. D. Ellis, N. A. Rorrer, K. P. Sullivan, M. Otto, J. E. McGeehan, Y. Román-Leshkov, N. Wierckx and G. T. Beckham, *Nat. Catal.*, 2021, **4**, 539–556.
10 K. Borg, A. Lennox, S. Kaufman, F. Tull, R. Prime, L. Rogers and E. Dunstan, *J. Clean. Prod.*, 2022, **344**, 131077.
11 Y. Chen, A. K. Awasthi, F. Wei, Q. Tan and J. Li, *Sci. Total Environ.*, 2021, **752**, 141772.
12 K. P. Gopinath, V. M. Nagarajan, A. Krishnan and R. Malolan, *J. Clean. Prod.*, 2020, **274**, 123031.
13 F. Zhang, Y. Zhao, D. Wang, M. Yan, J. Zhang, P. Zhang, T. Ding, L. Chen and C. Chen, *J. Clean. Prod.*, 2021, **282**, 124523.
14 T. Thiounn and R. C. Smith, *J. Polym. Sci.*, 2020, **58**, 1347–1364.
15 J. Zheng, M. Arifuzzaman, X. Tang, X. C. Chen and T. Saito, *Mater. Horiz.*, 2023, **10**, 1608–1624.
16 X. Zhao, B. Boruah, K. F. Chin, M. Đokić, J. M. Modak and H. S. Soo, *Adv. Mater.*, 2022, **34**, 2100843.
17 T.-W. Lin, O. Padilla-Vélez, P. Kaewdeewong, A. M. LaPointe, G. W. Coates and J. M. Eagan, *Chem. Rev.*, 2024, **124**, 9609–9632.
18 Z. O. G. Schyns and M. P. Shaver, *Macromol. Rapid Commun.*, 2021, **42**, 2000415.
19 Y. Liu, Z. Yu, B. Wang, P. Li, J. Zhu and S. Ma, *Green Chem.*, 2022, **24**, 5691–5708.
20 E. Morici and N. Tz. Dintcheva, *Polymers*, 2022, **14**, 4153.
21 Y. Tan, Y. Cheng, J. Xu and H. Wang, *Giant*, 2024, **19**, 100307.
22 H. T. Kim, J. K. Kim, H. G. Cha, M. J. Kang, H. S. Lee, T. U. Khang, E. J. Yun, D.-H. Lee, B. K. Song, S. J. Park, J. C. Joo and K. H. Kim, *ACS Sustainable Chem. Eng.*, 2019, **7**, 19396–19406.
23 D. Briassoulis, A. Pikasi and M. Hiskakis, *Polym. Degrad. Stabil.*, 2021, **183**, 109217.
24 L. Dai, N. Zhou, Y. Lv, Y. Cheng, Y. Wang, Y. Liu, K. Cobb, P. Chen, H. Lei and R. Ruan, *Prog. Energy Combust. Sci.*, 2022, **93**, 101021.
25 J. Choi, I. Yang, S.-S. Kim, S. Y. Cho and S. Lee, *Macromol. Rapid Commun.*, 2022, **43**, 2100467.
26 T. Y. A. Fahmy, Y. Fahmy, F. Mobarak, M. El-Sakhawy and R. E. Abou-Zeid, *Environ. Dev. Sustain.*, 2020, **22**, 17–32.
27 S. D. Anuar Sharuddin, F. Abnisa, W. M. A. Wan Daud and M. K. Aroua, *Energy Convers. Manage.*, 2016, **115**, 308–326.
28 Y. Shen, J. Wang, X. Ge and M. Chen, *Renew. Sustain. Energy Rev.*, 2016, **59**, 1246–1268.
29 H.-P. Schmidt, A. Anca-Couce, N. Hagemann, C. Werner, D. Gerten, W. Lucht and C. Kammann, *GCB Bioenergy*, 2019, **11**, 573–591.
30 R. C. Brown, *Processes*, 2021, **9**, 882.
31 A. S. Al-Fatesh, N. Y. A. AL-Garadi, A. I. Osman, F. S. Al-Mubaddel, A. A. Ibrahim, W. U. Khan, Y. M. Alanazi, M. M. Alrashed and O. Y. Alothman, *Fuel*, 2023, **344**, 128107.
32 H. Weldekidan, A. K. Mohanty and M. Misra, *ACS Environ. Au*, 2022, **2**, 510–522.
33 A. K. Panda, R. K. Singh and D. K. Mishra, *Renew. Sustain. Energy Rev.*, 2010, **14**, 233–248.
34 M. I. Jahirul, M. G. Rasul, D. Schaller, M. M. K. Khan, M. M. Hasan and M. A. Hazrat, *Energy Convers. Manage.*, 2022, **258**, 115451.
35 C. Zhuo and Y. A. Levendis, *J. Appl. Polym. Sci.*, 2014, **131**, 39931.
36 D. Jariwala, V. K. Sangwan, L. J. Lauhon, T. J. Marks and M. C. Hersam, *Chem. Soc. Rev.*, 2013, **42**, 2824–2860.
37 M. R. Benzigar, S. N. Talapaneni, S. Joseph, K. Ramadass, G. Singh, J. Scaranto, U. Ravon, K. Al-Bahily and A. Vinu, *Chem. Soc. Rev.*, 2018, **47**, 2680–2721.
38 Z. Yang, J. Ren, Z. Zhang, X. Chen, G. Guan, L. Qiu, Y. Zhang and H. Peng, *Chem. Rev.*, 2015, **115**, 5159–5223.
39 Z. Chen, X. Jiang, Y. Boyjoo, L. Zhang, W. Li, L. Zhao, Y. Liu, Y. Zhang, J. Liu and X. Li, *Electrochem. Energy Rev.*, 2024, **7**, 26.

40 Z. Zhang, Z. P. Cano, D. Luo, H. Dou, A. Yu and Z. Chen, *J. Mater. Chem. A*, 2019, **7**, 20985–21003.
41 A. Griffin, G. Chen, M. Robertson, K. Wang, Y. Xiang and Z. Qiang, *ACS Omega*, 2023, **8**, 15781–15789.
42 P. Zhang, M. He, W. Teng, F. Li, X. Qiu, K. Li and H. Wang, *Green Energy Environ.*, 2024, **9**, 1239–1256.
43 A. Griffin, M. Robertson, P. Frame, G. Ma, K. A. Green, Z. Han, S. E. Morgan, X. Gu, M. Wang and Z. Qiang, *J. Mater. Chem. A*, 2024, **12**, 13139–13152.
44 M. Robertson, B. Lamb, A. Griffin, L. He, B. Ma and Z. Qiang, *Mater. Horiz.*, 2025, **12**, 2935–2944.
45 S. J. Malode, S. Pandiaraj, A. Alodhayb and N. P. Shetti, *ACS Appl. Bio Mater.*, 2024, **7**, 752–777.
46 Y. Zhang, Z. Li, Z. Zhao, Y. Li, Z. Liu and S. Sun, *Carbon*, 2023, **212**, 118121.
47 A. Griffin, N. Smith, M. Robertson, B. Nunez, J. McCraw, H. Chen and Z. Qiang, *J. Chem. Educ.*, 2024, **101**, 1096–1105.
48 M. Robertson, A. Guillen Obando, B. Nunez, H. Chen and Z. Qiang, *ACS Appl. Eng. Mater.*, 2023, **1**, 165–174.
49 D. S. Su, S. Perathoner and G. Centi, *Chem. Rev.*, 2013, **113**, 5782–5816.
50 X. Liu and L. Dai, *Nat. Rev. Mater.*, 2016, **1**, 16064.
51 L. Zhang, C.-Y. Lin, D. Zhang, L. Gong, Y. Zhu, Z. Zhao, Q. Xu, H. Li and Z. Xia, *Adv. Mater.*, 2019, **31**, 1805252.
52 M. S. Ahmad and Y. Nishina, *Nanoscale*, 2020, **12**, 12210–12227.
53 A. Griffin, J. Wu, A. Smerigan, P. Smith, G. Adedigba, R. Shi, Y. Xiang and Z. Qiang, *Mater. Horiz.*, 2025, **12**, 3827–3840.
54 C. Perego and R. Millini, *Chem. Soc. Rev.*, 2013, **42**, 3956–3976.
55 N. Pal and A. Bhaumik, *RSC Adv.*, 2015, **5**, 24363–24391.
56 S. L. Candelaria, Y. Shao, W. Zhou, X. Li, J. Xiao, J.-G. Zhang, Y. Wang, J. Liu, J. Li and G. Cao, *Nano Energy*, 2012, **1**, 195–220.
57 L. Zu, W. Zhang, L. Qu, L. Liu, W. Li, A. Yu and D. Zhao, *Adv. Energy Mater.*, 2020, **10**, 2002152.
58 Y. Zhai, Y. Dou, D. Zhao, P. F. Fulvio, R. T. Mayes and S. Dai, *Adv. Mater.*, 2011, **23**, 4828–4850.
59 S. Pimenta and S. T. Pinho, *Waste Manage.*, 2011, **31**, 378–392.
60 M. Abdelhameed, M. Elbeh, N. S. Baban, L. Pereira, J. Matula, Y.-A. Song and K. B. Ramadi, *Green Chem.*, 2023, **25**, 1925–1937.
61 J. Gong, K. Yao, J. Liu, X. Wen, X. Chen, Z. Jiang, E. Mijowska and T. Tang, *Chem. Eng. J.*, 2013, **215–216**, 339–347.
62 D. Choi, D. Jang, H.-I. Joh, E. Reichmanis and S. Lee, *Chem. Mater.*, 2017, **29**, 9518–9527.
63 W. M. Qiao, S. H. Yoon, I. Mochida and J. H. Yang, *Waste Manage.*, 2007, **27**, 1884–1890.
64 W. M. Qiao, S. H. Yoon, Y. Korai, I. Mochida, S. Inoue, T. Sakurai and T. Shimohara, *Carbon*, 2004, **42**, 1327–1331.
65 W. M. Qiao, Y. Song, S.-H. Yoon, Y. Korai, I. Mochida, S. Yoshiga, H. Fukuda and A. Yamazaki, *Waste Manage.*, 2006, **26**, 592–598.
66 O. P. Krivoruchko, N. I. Maksimova, V. I. Zaikovskii and A. N. Salanov, *Carbon*, 2000, **38**, 1075–1082.
67 M. Jiang, X. Wang, W. Xi, H. Zhou, P. Yang, J. Yao, X. Jiang and D. Wu, *Chem. Eng. J.*, 2023, **461**, 141962.
68 A. R. Postema, H. De Groot and A. J. Pennings, *J. Mater. Sci.*, 1990, **25**, 4216–4222.
69 J. M. Younker, T. Saito, M. A. Hunt, A. K. Naskar and A. Beste, *J. Am. Chem. Soc.*, 2013, **135**, 6130–6141.
70 C. Zou, D. Wu, M. Li, Q. Zeng, F. Xu, Z. Huang and R. Fu, *J. Mater. Chem.*, 2010, **20**, 731–735.
71 C. D. Venkatachalam, S. Sekar, M. Sengottian, S. R. Ravichandran and P. Bhuvaneshwaran, *J. Energy Storage*, 2023, **67**, 107525.
72 D. Liu, L. Shi, Q. Dai, X. Lin, R. Mehmood, Z. Gu and L. Dai, *Trends Chem.*, 2024, **6**, 186–210.
73 L. Yaqoob, T. Noor and N. Iqbal, *ACS Omega*, 2022, **7**, 13403–13435.
74 T. Hees, F. Zhong, M. Stürzel and R. Mülhaupt, *Macromol. Rapid Commun.*, 2019, **40**, 1800608.
75 J.-P. Lange, *ACS Sustainable Chem. Eng.*, 2021, **9**, 15722–15738.
76 G. W. Coates and Y. D. Y. L. Getzler, *Nat. Rev. Mater.*, 2020, **5**, 501–516.
77 M. A. Hunt, T. Saito, R. H. Brown, A. S. Kumbhar and A. K. Naskar, *Adv. Mater.*, 2012, **24**, 2386–2389.
78 M. Robertson, A. Güillen Obando, J. Emery and Z. Qiang, *ACS Omega*, 2022, **7**, 12278–12287.
79 A. Griffin, P. Smith, P. Frame, K. Jones and Z. Qiang, *Adv. Sustainable Syst*, 2024, **8**, 2300332.
80 P. Smith, A. G. Obando, A. Griffin, M. Robertson, E. Bounds and Z. Qiang, *Adv. Mater.*, 2023, **35**, 2208029.
81 P. Smith, E. Bounds, K. Jones, A. Griffin, Z. Gunter and Z. Qiang, *MRS Communications*, 2024, **14**, 717–724.
82 P. J. Kim, H. D. Fontecha, K. Kim and V. G. Pol, *ACS Appl. Mater. Interfaces*, 2018, **10**, 14827–14834.
83 Y. Lian, M. Ni, Z. Huang, R. Chen, L. Zhou, W. Utetiwabo and W. Yang, *Chem. Eng. J.*, 2019, **366**, 313–320.
84 Q. Kong and J. Zhang, *Polym. Degrad. Stabil.*, 2007, **92**, 2005–2010.
85 Z. Xu, D. Sun, J. Xu, R. Yang, J. D. Russell and G. Liu, *ChemSusChem*, 2024, **17**, e202400474.
86 Z. Xu, F. Pan, M. Sun, J. Xu, N. E. Munyaneza, Z. L. Croft, G. Cai and G. Liu, *Proc. Natl. Acad. Sci. U.S.A.*, 2022, **119**, e2203346119.
87 N. E. Munyaneza, C. Posada, Z. Xu, V. De Altin Popiolek, G. Paddock, C. McKee and G. Liu, *Angew. Chem. Int. Ed.*, 2023, **62**, e202307042.
88 C. Marquez, C. Martin, N. Linares and D. De Vos, *Mater. Horiz.*, 2023, **10**, 1625–1640.
89 X. Yang, C. Li, G. Zhang and C. Yang, *J. Mater. Sci.*, 2015, **50**, 6649–6655.
90 C. Ma, J. Min, J. Gong, X. Liu, X. Mu, X. Chen and T. Tang, *Chemosphere*, 2020, **253**, 126755.
91 F. G. F. de Paula, M. C. M. de Castro, P. F. R. Ortega, C. Blanco, R. L. Lavall and R. Santamaría, *Microporous Mesoporous Mater.*, 2018, **267**, 181–184.
92 S. Ma, S. Tang and Y. Zhao, *Chem. Eng. J.*, 2024, **498**, 155460.
93 Y.-H. Chung and S. Jou, *Mater. Chem. Phys.*, 2005, **92**, 256–259.
94 H. Song, X. Liu, B. Wang, Z. Tang and S. Lu, *Sci. Bull.*, 2019, **64**, 1788–1794.
95 V. G. Pol, *Environ. Sci. Technol.*, 2010, **44**, 4753–4759.
96 C. Bharadwaj, R. Purbey, D. Bora, P. Chetia, U. Maheswari R, R. Duarah, K. Dutta, E. R. Sadiku, K. Varaprasad and J. Jayaramudu, *Mater. Today Sustain.*, 2024, **27**, 100936.
97 J. Diao, Y. Hu, Y. Tian, R. Carr and T. S. Moon, *Cell Rep.*, 2023, **42**, 111908.
98 N. Vora, P. R. Christensen, J. Demarteau, N. R. Baral, J. D. Keasling, B. A. Helms and C. D. Scown, *Sci. Adv.*, **7**, eabf0187.
99 Z. Jia, L. Gao, L. Qin and J. Yin, *RSC Sustainability*, 2023, **1**, 2135–2147.
100 A. Mirjalili, B. Dong, P. Pena, C. S. Ozkan and M. Ozkan, *Energy Storage*, 2020, **2**, e201.
101 X. Yuan, N. M. Kumar, B. Brigljević, S. Li, S. Deng, M. Byun, B. Lee, C. S. K. Lin, D. C. W. Tsang, K. B. Lee, S. S. Chopra, H. Lim and Y. S. Ok, *Green Chem.*, 2022, **24**, 1494–1504.
102 B. Chen, J. Ren, Y. Song, P. He, H. Bai, Z. Fan, R. Niu and J. Gong, *ACS Sustainable Chem. Eng.*, 2022, **10**, 16427–16439.

103 S. Li, M.-K. Cho, S. Deng, J. Wang and K. B. Lee, *Chem. Eng. J.*, 2024, **494**, 152931.
104 A. R. Kamali, J. Yang and Q. Sun, *Appl. Surf. Sci.*, 2019, **476**, 539–551.
105 E. Salama, S. Mohamed, M. Samy, K. Mensah, M. Ossman, M. F. Elkady and H. Shokry Hassan, *RSC Adv.*, 2024, **14**, 1977–1983.
106 A. Joseph Berkmans, M. Jagannatham, S. Priyanka and P. Haridoss, *Waste Manage.*, 2014, **34**, 2139–2145.
107 Y. Wu, G. Ma, A. Zhang, W. Gu, J. Wei and R. Wang, *ACS Omega*, 2022, **7**, 38037–38044.
108 P. S. Roy, G. Garnier, F. Allais and K. Saito, *ChemSusChem*, 2021, **14**, 4007–4027.
109 S. L. Wong, N. Ngadi, T. A. T. Abdullah and I. M. Inuwa, *Renew. Sustain. Energy Rev.*, 2015, **50**, 1167–1180.
110 J. L. Self, A. J. Zervoudakis, X. Peng, W. R. Lenart, C. W. Macosko and C. J. Ellison, *JACS Au*, 2022, **2**, 310–321.
111 Y. V. Vazquez and S. E. Barbosa, *Waste Manage.*, 2016, **53**, 196–203.
112 J. Qian, C. B. Dunn and Z. Qiang, *Macromol. Chem. Phys.*, 2023, **224**, 2300291.
113 T. Kwon, H. Jeong, M. Kim, S. Jung and I. Ro, *Langmuir*, 2024, **40**, 17212–17238.
114 M. G. Davidson, R. A. Furlong and M. C. McManus, *J. Clean. Prod.*, 2021, **293**, 126163.
115 L. Dai, O. Karakas, Y. Cheng, K. Cobb, P. Chen and R. Ruan, *Chem. Eng. J.*, 2023, **453**, 139725.
116 M. Kusenberg, A. Eschenbacher, L. Delva, S. De Meester, E. Delikonstantis, G. D. Stefanidis, K. Ragaert and K. M. Van Geem, *Fuel Process. Technol.*, 2022, **238**, 107474.
117 M. Larrain, S. Van Passel, G. Thomassen, U. Kresovic, N. Alderweireldt, E. Moerman and P. Billen, *J. Clean. Prod.*, 2020, **270**, 122442.
118 H. Jeswani, C. Krüger, M. Russ, M. Horlacher, F. Antony, S. Hann and A. Azapagic, *Sci. Total Environ.*, 2021, **769**, 144483.
119 D. Yao, H. Li, B. C. Mohan, A. K. Prabhakar, Y. Dai and C.-H. Wang, *ACS Sustainable Chem. Eng.*, 2022, **10**, 1125–1136.
120 S. Belbessai, E.-H. Benyoussef, F. Gitzhofer and N. Abatzoglou, *Chem. Eng. J. Adv.*, 2022, **12**, 100424.
121 W. A. Algozeeb, P. E. Savas, D. X. Luong, W. Chen, C. Kittrell, M. Bhat, R. Shahsavari and J. M. Tour, *ACS Nano*, 2020, **14**, 15595–15604.
122 J. Ma, J. Liu, J. Song and T. Tang, *RSC Adv.*, 2018, **8**, 2469–2476.
123 Y. Wen, K. Kierzek, X. Chen, J. Gong, J. Liu, R. Niu, E. Mijowska and T. Tang, *Waste Manage.*, 2019, **87**, 691–700.
124 X. Zhou, P. He, W. Peng, J. Zhou, M. Jiang, H. Zhang and W. Dong, *Resour. Conserv. Recycl.*, 2023, **193**, 106988.
125 A. Veksha, A. Giannis and V. W.-C. Chang, *J. Anal. Appl. Pyrolysis.*, 2017, **124**, 16–24.
126 P. Shieh, W. Zhang, K. E. L. Husted, S. L. Kristufek, B. Xiong, D. J. Lundberg, J. Lem, D. Veysset, Y. Sun, K. A. Nelson, D. L. Plata and J. A. Johnson, *Nature*, 2020, **583**, 542–547.
127 Y. Zhang, L. Zhang, G. Yang, Y. Yao, X. Wei, T. Pan, J. Wu, M. Tian and P. Yin, *J. Mater. Sci. Technol.*, 2021, **92**, 75–87.
128 F. M. Uhl, G. F. Levchik, S. V. Levchik, C. Dick, J. J. Liggat, C. E. Snape and C. A. Wilkie, *Polym. Degrad. Stabil.*, 2001, **71**, 317–325.
129 Y. Li, Y. Fan and J. Ma, *Polym. Degrad. Stabil.*, 2001, **73**, 163–167.
130 G. F. Levchik, K. Si, S. V. Levchik, G. Camino and C. A. Wilkie, *Polym. Degrad. Stabil.*, 1999, **65**, 395–403.
131 R. Janus, A. Wach, P. Kuśtrowski, B. Dudek, M. Drozdek, A. M. Silvestre-Albero, F. Rodríguez-Reinoso and P. Cool, *Langmuir*, 2013, **29**, 3045–3053.
132 J. Sun, G. Wu and Q. Wang, *J. Mater. Sci.*, 2005, **40**, 663–668.
133 B. Wang, Y. Wang, S. Du, J. Zhu and S. Ma, *Mater. Horiz.*, 2023, **10**, 41–51.
134 S. Xiao, S. Liu, J. Zhang and Y. Wang, *J. Power Sources*, 2015, **293**, 119–126.
135 K. M. Wyss, J. T. Li, P. A. Advincula, K. V. Bets, W. Chen, L. Eddy, K. J. Silva, J. L. Beckham, J. Chen, W. Meng, B. Deng, S. Nagarajaiah, B. I. Yakobson and J. M. Tour, *Adv. Mater.*, 2023, **35**, 2209621.
136 X. Zhou, L. Zhu, Y. Yang, L. Xu, X. Qian, J. Zhou, W. Dong and M. Jiang, *Chemosphere*, 2022, **300**, 134552.
137 A. G. Obando, M. Robertson, C. Umeojiakor, P. Smith, A. Griffin, Y. Xiang and Z. Qiang, *J. Mater. Res.*, 2024, **39**, 115–125.
138 D. Torres, S. Pérez-Rodríguez, L. Cesari, C. Castel, E. Favre, V. Fierro and A. Celzard, *Carbon*, 2021, **183**, 12–33.
139 R. Liu, Y. Shi, Y. Wan, Y. Meng, F. Zhang, D. Gu, Z. Chen, B. Tu and D. Zhao, *J. Am. Chem. Soc.*, 2006, **128**, 11652–11662.
140 H. Ishida, in *Handbook of Benzoxazine Resins*, eds. H. Ishida and T. Agag, Elsevier, Amsterdam, 2011, pp. 3–81.
141 Y. Xu, L. Guo, H. Zhang, H. Zhai and H. Ren, *RSC Adv.*, 2019, **9**, 28924–28935.
142 W.-H. Kuan, Y.-S. Hu, C.-Y. Chiu, K.-Y. Hung and S.-S. Chou, *Catalysts*, 2021, **11**, 783.
143 I. Tiwari, P. Sharma and L. Nebhani, *Mater. Today Chem.*, 2022, **23**, 100734.
144 C. Shaer, L. Oppenheimer, A. Lin and H. Ishida, *Polymers*, 2021, **13**, 3775.
145 P. Sharma, V. Tanwar, I. Tiwari, P. P. Ingole and L. Nebhani, *Energy Fuels*, 2023, **37**, 7445–7467.
146 N. Siraj, S. A. R. Hashmi and S. Verma, *Polym. Adv. Technol.*, 2022, **33**, 3049–3077.
147 T. P. McNicholas, A. Wang, K. O'Neill, R. J. Anderson, N. P. Stadie, A. Kleinhammes, P. Parilla, L. Simpson, C. C. Ahn, Y. Wang, Y. Wu and J. Liu, *J. Phys. Chem. C*, 2010, **114**, 13902–13908.
148 C. H. J. Kim, H. Zhang and J. Liu, *2D Mater.*, 2015, **2**, 024006.
149 M. Moos, J. Best, S. Flauder, S. R. Nutt, N. Langhof and S. Schafföner, *J. Polym. Sci.*, DOI:10.1002/pol.20250057.
150 D. Veazey, T. Hsu and E. D. Gomez, *J. Appl. Polym. Sci.*, 2017, **134**, 44441.
151 S. M. Saufi and A. F. Ismail, *Carbon*, 2004, **42**, 241–259.
152 W. Qiu, J. E. Leisen, Z. Liu, W. Quan and W. J. Koros, *Angew. Chem. Int. Ed.*, 2021, **60**, 22322–22331.
153 W. Guzman, A. Griffin, M. Robertson, W. L. Jarrett, Z. Qiang and J. S. Wiggins, *ACS Appl. Nano Mater.*, 2023, **6**, 14957–14966.
154 J. Su, S. Zhou, R. Li, Z. Xiao and H. Cui, *Carbon*, 2015, **93**, 1081.
155 S. Utekar, S. V K, N. More and A. Rao, *Compos. Part B Eng.*, 2021, **207**, 108596.
156 A. Griffin, Y. Guo, Z. Hu, J. Zhang, Y. Chen and Z. Qiang, *Polym. Compos.*, 2022, **43**, 5747–5766.
157 J. Howarth, S. S. R. Mareddy and P. T. Mativenga, *J. Clean. Prod.*, 2014, **81**, 46–50.
158 J. Zhang, V. S. Chevali, H. Wang and C.-H. Wang, *Compos. Part B Eng.*, 2020, **193**, 108053.
159 A. Lefeuvre, S. Garnier, L. Jacquemin, B. Pillain and G. Sonnemann, *Resour. Conserv. Recycl.*, 2019, **141**, 30–39.
160 A. Lefeuvre, S. Garnier, L. Jacquemin, B. Pillain and G. Sonnemann, *Resour. Conserv. Recycl.*, 2017, **125**, 264–272.

161 Y. Shen, S. E. Apraku and Y. Zhu, *Green Chem.*, 2023, **25**, 9644–9658.
162 S. R. Naqvi, H. M. Prabhakara, E. A. Bramer, W. Dierkes, R. Akkerman and G. Brem, *Resour. Conserv. Recycl.*, 2018, **136**, 118–129.
163 L. O. Meyer, K. Schulte and E. Grove-Nielsen, *J. Compos. Mater.*, 2009, **43**, 1121–1132.
164 Q. Zhao, J. Jiang, C. Li and Y. Li, *Polym. Degrad. Stabil.*, 2020, **179**, 109268.
165 B. Wang, X. Wang, N. Xu, Y. Shen, F. Lu, Y. Liu, Y. Huang and Z. Hu, *Compos. Sci. Technol.*, 2021, **203**, 108589.
166 W. Nie, J. Liu, W. Liu, J. Wang and T. Tang, *Polym. Degrad. Stabil.*, 2015, **111**, 247–256.
167 X. Huan, T. Wu, J. Yan, X. Jia, L. Zu, G. Sui and X. Yang, *Compos. Part B Eng.*, 2021, **211**, 108656.
168 M. Das, R. Chacko and S. Varughese, *ACS Sustainable Chem. Eng.*, 2018, **6**, 1564–1571.
169 Y. Wang, J. Li, X. Zhou, T. Wang, Q. Zhao, H. Zhang, Y. Wang and X. Hou, *Compos. Sci. Technol.*, 2020, **199**, 108342.
170 L. Zhang, W. Liu, H. Jiang, X. Zhang, Y. Shang, C. Jiang, X. Wang, G. Qi, B. Li, P. Xu and J. Qiao, *Compos. Sci. Technol.*, 2023, **231**, 109824.
171 A. Griffin, M. Robertson, Z. Gunter, A. Coronado, Y. Xiang and Z. Qiang, *Ind. Eng. Chem. Res.*, 2024, **63**, 19398–19417.
172 B. Hernández, P. Kots, E. Selvam, D. G. Vlachos and M. G. Ierapetritou, *ACS Sustainable Chem. Eng.*, 2023, **11**, 7170–7181.
173 X. Qin, C. Yu, W. Zhou, Z. Xu, J. Chang and X. Wang, *J. Mater. Chem. A*, 2025, **13**, 12828–12854.
174 S. A. Theofanidis, E. Delikonstantis, V.-L. Yfanti, V. V. Galvita, A. A. Lemonidou and K. Van Geem, *Waste Manage.*, 2025, **193**, 155–170.
175 Q. Dong, Y. Yao, S. Cheng, K. Alexopoulos, J. Gao, S. Srinivas, Y. Wang, Y. Pei, C. Zheng, A. H. Brozena, H. Zhao, X. Wang, H. E. Toraman, B. Yang, I. G. Kevrekidis, Y. Ju, D. G. Vlachos, D. Liu and L. Hu, *Nature*, 2022, **605**, 470–476.
176 Q. Dong, A. D. Lele, X. Zhao, S. Li, S. Cheng, Y. Wang, M. Cui, M. Guo, A. H. Brozena, Y. Lin, T. Li, L. Xu, A. Qi, I. G. Kevrekidis, J. Mei, X. Pan, D. Liu, Y. Ju and L. Hu, *Nature*, 2023, **616**, 488–494.
177 B. Deng, L. Eddy, K. M. Wyss, C. S. Tiwary and J. M. Tour, *Nat. Rev. Clean Technol.*, 2025, **1**, 32–54.
178 S. Y. Foong, Y. H. Chan, P. N. Y. Yek, S. S. M. Lock, B. L. F. Chin, C. L. Yiin, J. C.-W. Lan and S. S. Lam, *Chem. Eng. J.*, 2024, **491**, 151942.
179 M. Robertson, A. Guillen-Obando, A. Barbour, P. Smith, A. Griffin and Z. Qiang, *Nat. Commun.*, 2023, **14**, 639.
180 A. Griffin, P. Frame, Y. Xiang and Z. Qiang, *ACS Omega*, 2025, **10**, 11554–11561.

Table 1. Summary of important parameters for upcycling various plastic wastes into carbon materials.

Precursor	Carbonization methodology	Carbon yield (wt%)	Type of carbon	Target Application	Ref.
LLDPE	Catalytic carbonization with nickel (III) oxide and PVC resin	64	CNTs, carbon nanofibers, and amorphous carbon	Micropollutant sorbents	61
LLDPE (cling wrap and poly gloves)	Thermal oxidation	50	Graphitic carbon	-	62
LLDPE	Chlorosulphonic acid crosslinking and pyrolysis	75	Carbon fiber	-	68
PS	$CCl_3/AlCl_3$ treatment and pyrolysis	40	HPCs	-	70
PE	Sulfonation-based crosslinking and pyrolysis	-	Patterned CFs	-	77
PP (surgical masks)	Sulfonation-based crosslinking and pyrolysis	58	Carbon fibers	Joule heating, micropollutant/CO_2 sorbents	48,78
PP (textiles)	Sulfonation-based crosslinking and pyrolysis	59	Woven carbon fiber mats	Joule heating	79
LDPE (plastic bags)	Microwave-assisted sulfonation	50	Porous, sulfonated carbon	Interlayer for lithium-sulfur batteries	82
PE (plastic bags)	Carbonization with flame-retardant agent	~45	HPCs	Supercapacitor electrodes	83
PE	Catalytic carbonization with maleated PP	80	Straight and helical CNTs	-	84
PS	$CCl_3/AlCl_3$ treatment and pyrolysis	40	HPCs	Anodes for lithium-ion batteries	89
PS foam	Pyrolysis with Fe_2O_3	46	3D-HPCs	Supercapacitor electrodes	90
PS foam	Pyrolysis	-	Activated carbon	Supercapacitor electrodes and Micropollutant sorbents	91
PS microplastics	Nitrification and pyrolysis	-	Fe/Mo-doped sponge carbon	Fenton reaction catalysts	92
PS	Catalytic carbonization with iron nanoparticles	-	CNTs	-	93
PS	Solvothermal method in DCM and nitric acid	60-85	Carbon dots	Multi-color light-emitting diodes	94
PS foam	Thermal dissociation under autogenic pressure	-	Paramagnetic carbon microspheres	-	95
PET bottles	Pyrolysis	-	Microporous carbon and graphene oxide	Supercapacitor electrodes	100
PET bottles	Pyrolysis	-	Porous carbon	CO_2 sorbents	101
PET bottles	Solvothermal synthesis with Ca-MOF and calcium chloride followed by pyrolysis	64	PCCs	Interfacial solar-driven water–thermoelectricity cogeneration	102
PET bottles	Autogenic pressure carbonization	~15	Porous carbon	CO_2 sorbents	103
PET bottles	Pyrolysis with molten NaCl	16	Graphitic nanosheets	-	104
PET cups	Pyrolysis with catalyst prepared from citric acid combustion of anhydrous iron(III) chloride and aluminum nitrate nonahydrate	-	Graphene	-	105
PET bottles	Rotating cathode arc discharge technique	-	Nanosized, ultrafine solid carbon spheres and MWCNTs	-	106
PET fibers	Micrwave irradiation and hydrothermall method with urea and pyromellitic acid	-	Carbon dots	Fluorescence probe	107
PE:PP	Sulfonation-based crosslinking and pyrolysis	73	3D-printed structured carbon	Joule heaters and catalyst supports for electrified hydrogen production	53
PP:LDPE:PS:PET	Pyrolysis with bimetallic catalysts	30	Porous carbon	Micropollutant sorbents	119

PE:PP:PC/PET:metal/wood	In-line pyrolysis with nickel-upgraded slug oxide	46	Carbon nanofilaments	-	120
HDPE:PP:PET:LDPE:PS:PVC	FJH	22	Graphene	-	121
PP:LDPE:HDPE:PS:PET:PVC	Pressurized carbonization with magnesium oxide	33	Porous carbon	-	122
PE:PP:PS:PET:PVC containing moisture and ash	Pyrolysis with OMMT	60	Porous carbon nanosheets	Supercapacitor electrodes	123
PP:LDPE:HDPE:PS	Autogenic pressure pyrolysis	49	Carbon microspheres	-	124
LDPE:PP:PS:PET	Pyrolysis with nickel on calcium carbonate support	22	MWCNT and carbon nanocages	-	125
Crosslinked PU foam	Pyrolysis with potassium carbonate	28	Porous carbon	Polysulfide reservoirs for lithium-sulfur batteries	134
Crosslinked PU	FJH with ferrocene and iron(III) chloride-based catalysts	~9	Graphitic 1D carbon	-	135
Crosslinked PU foam	Autogenic atmosphere pyrolysis	55	Porous carbon	Supercapacitor electrodes	136
Crosslinked PE foam	Stabilization with fuming sulfuric acid and pyrolysis	50	Porous carbon	CO_2 sorbents	137
Phenolic resin waste	Microwave-assisted carbonization with KOH or H_3PO_4	-	Porous carbon	Micropollutant sorbents	142
Polybenzoxazine	Thermal oxidation and pyrolysis	12	Nitrogen-doped carbon	Supercapacitor electrodes	145
PEEK	Pyrolysis	-	Porous carbon	Hydrogen storage	147
PEEK	Pyrolysis	-	Porous carbon	Supercapacitor electrodes	148
PEEK	Pyrolysis	54	Carbon fiber	Aerospace/construction	149
PEKK	Pyrolysis	65	Carbon fiber	Aerospace/construction	149
CF-BMI composite	Chemical degradation with acetic acid/$Ca(NO_3)_2$ and pyrolysis	-	Nitrogen-doped carbon	Catalysts for the aerobic oxidation of HMF to DFF	164

Data availability

No primary research results, software or code have been included and no new data were generated or analysed as part of this review.